Canadian Mineralogist
Vol. 19, pp. 269-277 (1981)

Ca–Fe–Si SKARNS CONTAINING BABINGTONITE: FIRST KNOWN OCCURRENCE IN AUSTRALIA

M.J. GOLE*

School of Earth Sciences, Macquarie University, North Ryde, New South Wales 2113, Australia

ABSTRACT

At Black Perry Mountain, southern New South Wales, skarns containing hedenbergite (Hed), andradite (And), ilvaite, quartz (Qtz), calcite (Cal), magnetite, actinolite, epidote, babingtonite and stilpnomelane extend for 4 km away from an exposed granite contact. All skarn outcrops contain similar mineral assemblages except for babingtonite assemblages. The main minerals have nearly pure Ca–Fe end-member compositions and have similar compositions throughout the skarns. This is the first occurrence of babingtonite in Australia. Its formula is $Na_{0.04}Ca_{2.00}Fe^{2+}{}_{0.76}Mn_{0.15}Mg_{0.12}Fe^{3+}{}_{0.99}Al_{0.04}Si_{4.96}O_{14}(OH)_{0.96}$; its cell data are *a* 7.49(1), *b* 11.83(1), *c* 6.72(1) Å, α 95.3(1)°, β 92.3(1)° and γ 103.1 (1)°, and its optical properties are n_α 1.716(2), n_β 1.731(2), n_γ 1.750(2), $Z \Lambda c$ 43(3)° and $2V_\alpha$ 69 (3)°. The first-formed assemblage (Hed–And–Qtz–Cal) occurs in all skarn outcrops, which suggests that these skarns experienced similar peak metamorphic conditions. Thus the granite would be buried not too deeply below the skarns. Assemblages containing ilvaite, babingtonite, actinolite and stilpnomelane developed after the formation of Hed–And–Qtz–Cal. Experimental data indicate that Hed–And–Qtz–Cal formed between about 580 and 640°C, with $f(O_2)$ just above the upper $f(O_2)$ stability of graphite and $X(CO_2)$ between ~ 0.1 and ~ 0.3.

Keywords: skarn, hedenbergite, andradite, babingtonite, ilvaite, New South Wales, Australia.

SOMMAIRE

Au mont Black Perry (Nouvelles Galles du Sud méridionales), on trouve des skarns à hédenbergite (Hed), andradite (And), ilvaïte, quartz (Qtz), calcite (Cal), magnétite, actinote, épidote, babingtonite et stilpnomélane jusqu'à 4 km du contact exposé avec un massif granitique. Tous les affleurements de skarn montrent pareils assemblages de minéraux, sauf ceux où se présente la babingtonite. Les phases essentielles sont toutes proches du pôle Ca–Fe, et chacune est de composition uniforme dans toute l'étendue du skarn. La babingtonite, signalée ici pour la première fois en Australie, répond à la formule $Na_{0.04}Ca_{2.00}Fe^{2+}{}_{0.76}Mn_{0.15}Mg_{0.12}Fe^{3+}{}_{0.99}Al_{0.04}Si_{4.96}O_{14}(OH)_{0.96}$. Paramètres réticulaires: *a* 7.49(1), *b* 11.83(1), *c* 6.72(1) Å, α 95.3(1)°, β 92.3(1)°, γ 103.1(1)°; propriétés optiques: n_α 1.716(2), n_β 1.731(2), n_γ 1.750(2), $Z \Lambda$ c 43(3)°, $2V_\alpha$ 69(3)°. La présence, dans tous les affleurements, du premier assemblage formé (Hed–And–Qtz–Cal) refléterait l'uniformité de l'intensité maximum du métamorphisme. Le massif granitique se trouverait donc enfoui à faible profondeur sous les skarns. Les assemblages à ilvaïte, babingtonite, actinote et stilpnomélane sont tardifs. D'après les données expérimentales, l'association Hed + And + Qtz + Cal s'est formée entre 580 et 640°C, la fugacité d'oxygène étant légèrement supérieure à la stabilité du graphite, et la fraction molaire $X(CO_2)$ se situant entre ~ 0.1 et ~ 0.3.

(Traduit par la Rédaction)

Mots-clés: skarn, hédenbergite, andradite, babingtonite, ilvaïte, Nouvelles Galles du Sud, Australie.

INTRODUCTION

At Black Perry Mountain, southern New South Wales (Fig. 1), Ca–Fe–Si skarns composed predominately of hedenbergite, andradite, ilvaite, quartz and calcite contain minor to trace amounts of magnetite, actinolite, epidote, babingtonite and stilpnomelane. These skarns contain the first known occurrence of babingtonite in Australia.

The main skarn minerals have almost Ca–Fe end-member compositions and contain very little Al_2O_3 and MgO. These latter components are important constituents of many other skarns (*e.g.*, Brock 1972, Morgan 1975, Kwak 1978). Their low concentration in the Black Perry Mountain skarns is an important contributing factor in the occurrence of babingtonite at this locality. Burt (1971a) listed only six localities in the world where babingtonite is present in skarns; he showed that it occurs most commonly in low-grade alteration assemblages in metabasalts. This report describes the Black Perry Mountain skarns and their mineralogy. From experimental data on the system Ca–Fe–

*Present address: Department of Geology, Georgia State University, University Plaza, Atlanta, Georgia 30303, U.S.A.

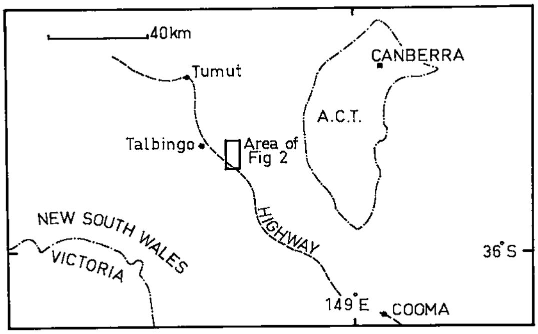

FIG. 1. Locality map showing Black Perry Mountain area.

Si–C–O–H, the peak metamorphic conditions under which the earliest skarn assemblage formed are estimated.

GEOLOGICAL AND MINERALOGICAL RELATIONSHIPS

The Ca–Fe–Si skarns, invariably associated with marble, appear to be concordant within a sequence of predominantly clastic metasedimentary rocks of middle Silurian age (Adamson 1955) that form a large embayment into the Bogong Granite (Fig. 2). The skarns extend for 4 km away from the granite–metasediment contact, and the most southerly outcrop is approximately equidistant (3 km) from either side of the embayment. Vertical relief along the main skarn outcrop is approximately 200 m whereas the vertical distance between outcrops is over 350 m.

Hedenbergite and andradite comprise over 70% of the Ca–Fe–Si skarns, with hedenbergite usually predominating. Monomineralic hedenbergite rocks occur with both parallel and radiating aggregates of bladed crystals up to 3 cm long. Andradite occurs as isolated grains in most hedenbergite rocks and also in monomineralic and andradite–quartz assemblages in patches up to several metres across. Coarse grained aggregates (grains up to 2–3 cm long) and veins up to 10 cm wide, both containing andradite with ilvaite, quartz and minor calcite, are common. Ilvaite, quartz and calcite are disseminated throughout the skarns and also occur in coarse grained monomineralic patches, as well as in quartz–ilvaite–calcite, quartz–ilvaite and ilvaite–calcite assemblages. Calcite, a minor phase in many outcrops, is absent in many samples of hand-specimen size. Magnetite occurs as fine grained ragged aggregates in complex intergrowths with other minerals, notably hedenbergite. Boulders consisting of coarse grained euhedral magnetite with andradite and quartz occur 100 m north of Black Perry Mountain. but this assemblage was not observed in outcrop.

Actinolite and stilpnomelane are minor phases, and epidote is rare except near the contact with epidote skarn (see below). Actinolite generally occurs in veins and as fibrous aggregates either

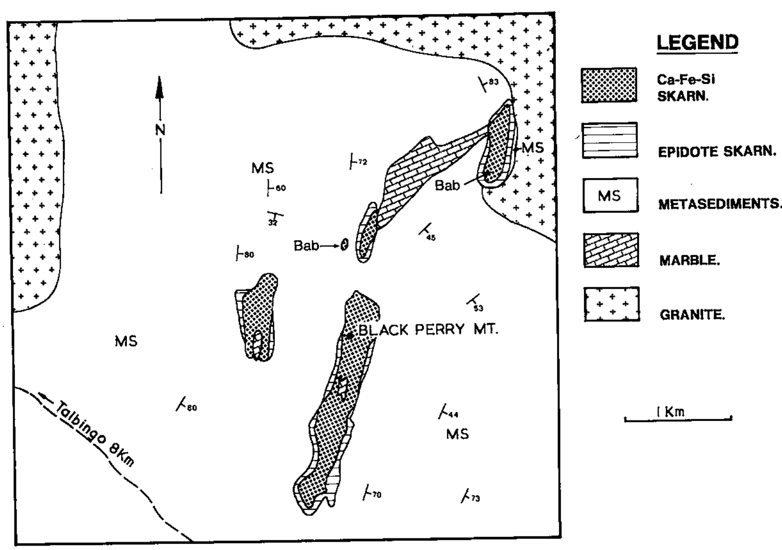

FIG. 2. Geology of the Black Perry Mountain area showing Ca–Fe–Si skarn distribution.

within hedenbergite grains or cutting across hedenbergite–quartz grain boundaries. Although these veins are generally monomineralic, ilvaite, andradite and, rarely, magnetite may form part of the vein assemblage. Both green and brown stilpnomelane occur as ragged rosettes within quartz and calcite in many hedenbergite-rich assemblages.

The only mineral that appears restricted in its field occurrence is babingtonite. It was found only near the granite contact and as a trace amount within a small outcrop northwest of Black Perry Mountain (Fig. 2).

Epidote-rich skarns containing additional quartz with minor garnet, pyroxene, magnetite, calcite and rare veins of hematite crop out in most places between Ca–Fe–Si skarns and metasediments. The boundary between Ca–Fe–Si skarns and epidote skarns is gradational, but the epidote skarn–metasediment contact is sharp.

The marble, unlike the skarns, contains trace amounts of carbonaceous material, although no graphite was detected. Contacts between marble and the skarns are sharp and in places may be marked by 2–3-cm-wide monomineralic bands of hedenbergite against the marble and andradite against the skarns. Ilvaite occurs rarely within the marble, 1–2 cm from the contact.

Wollastonite occurs with calcite and vesuvianite in coarse grained patches within the metasediments 500 m northwest of the westernmost Ca–Fe–Si skarn outcrop. However, no mineralogical variation was observed in the metasediments that could be used to establish temperature gradients away from the exposed granite–metasediment contacts.

Mineral-assemblage zonation, such as that studied by Burt (1974) and common in other Ca–Fe–Si skarns, is not present within the Ca–Fe–Si skarns at Black Perry Mountain. The only exception is the 2–3-cm-wide monomineralic bands of hedenbergite and andradite occurring at the contact between the Ca–Fe–Si skarns and marble.

TABLE 1. CHEMICAL ANALYSES OF MINERALS FROM BLACK PERRY MOUNTAIN[a]

Sample No.	1	2	3	4	5	6	7
SiO_2	48.5	35.7	35.2	29.4	52.3	52.5	44.2
TiO_2	0.01	0.02	0.08	0.01	0.01	0.00	0.03
Al_2O_3	0.35	1.41	0.45	0.27	0.33	0.78	11.6
Fe_2O_3	1.4	28.6	31.0[b]	18.9	13.8	0.9[c]	-
FeO	24.2	0.2	-	31.2	9.6	23.8	31.4[d]
MnO	1.44	0.13	0.80	2.24	1.91	0.64	2.36
MgO	1.82	1.16	0.01	1.00	0.84	8.41	4.68
CaO	21.6	32.9	32.7	14.0	19.7	11.9	0.53
Na_2O	0.35	-	-	0.19	0.23	0.07	0.31
K_2O	0.00	-	-	0.01	0.00	0.02	1.60
H_2O^+	-	-	-	1.8	1.5	-	-
H_2O^-	-	-	-	0.05	0.20	-	-
Total	99.67	100.12	100.24	99.07	100.42	99.02	96.71
ATOMIC PROPORTIONS:							
O + OH	6	24	24	9	15	23	11
Si	1.98	5.97	5.95	2.02	4.96	7.88	3.33
Al	0.02	0.03	0.05	0.00	0.04	0.12	0.67
	2.00	6.00	6.00	2.02	5.00	8.00	4.00
Al	0.00	0.25	0.04	0.02	0.00	0.02	0.36
Ti	0.00	0.00	0.01	0.00	0.00	0.00	0.00
Fe^{3+}	0.04	3.60	3.94	0.97	0.99	0.10	-
Fe^{2+}	0.83	0.03	-	1.79	0.76	2.99	1.98
Mn	0.05	0.02	0.11	0.13	0.15	0.08	0.15
Mg	0.11	0.29	0.00	0.10	0.12	1.88	0.53
Ca	0.95	5.90	5.92	1.03	2.00	1.91	0.04
Na	0.03	-	-	0.03	0.04	0.02	0.05
K	0.00	-	-	0.00	0.00	0.00	0.15
OH	-	-	-	0.82	0.96	-	-
	2.01	10.9	10.02	4.89	5.02	7.00	3.26

a. Analyses 1, 2, 4 and 5 done at Macquarie University by XRF except for Na_2O (flame photometry), FeO (sodium metavanadate titration) and H_2O (gravimetry). These minerals, crushed to 150-200μ, were separated to >98% purity by magnetic, heavy liquid and hand-picking techniques. Analyses 3, 6, and 7 done at The University of Western Australia by electron microprobe using the correction procedure of Bence & Albee (1968): b. Fe_2O_3 assuming B site = 4.00: c. Fe_2O_3 estimated by method of Papike *et al.* (1974): d. All Fe as FeO: - = not determined.

1. Hedenbergite from andradite-hedenbergite-ilvaite-magnetite rock: 2. Andradite from monomineralic rock: 3. Andradite from actinolite-andradite-ilvaite vein: 4. Ilvaite from ilvaite-babingtonite-minor calcite and epidote rock: 5. Babingtonite from 4 above: 6. Ferro-actinolite from 3 above: 7. Stilpnomelane

MINERAL COMPOSITIONS

The compositions of the main mineral species are similar in all the main skarn outcrops. The minor compositional variations show no correlation with distance fgrom the exposed granite or with position within Ca–Fe–Si skarn outcrops. Hedenbergites from nine samples from widely scattered localities show a range in Fe/(Fe+Mg) of 0.70 to 0.95, although the range shown by eight of these hedenbergites is only 0.89 to 0.95. The most Mg-rich hedenbergite occurs as an inclusion within an andradite grain. A typical analysis of hedenbergite (Table 1, No. 1) shows that the amounts of the diopside and johannsenite components are small. Most garnets are slightly anisotropic and contain discrete compositional zones. Electron-microprobe analyses show that the zoning in one such grain varies from $And_{56}Gros_{43}$ to And_{99}, with minor amounts of other garnet end-member components present. Grossular-rich zones, however, make up a relatively small proportion of garnet grains, as shown by the analyses of six bulk garnet samples from widely spaced localities that yielded compositions from And_{84} to And_{93} (see Table 1, No. 2 for a representative analysis). Isotropic and compositionally homogeneous garnets occurring in actinolite veinlets have high concentrations of the andradite component and contain slightly higher spessartine but significantly lower pyrope components than anisotropic garnets (Table 1, No. 3). Ilvaite contains very little Mg and small amounts of Mn (Table 1, No. 4), which can readily substitute into the ilvaite structure (Leonard *et al.* 1962). In babingtonite, substitutions similar to those in ilvaite are possible; Mn can apparently substitute to a greater extent, although rarely with nearly complete substitution for Fe^{2+} (Vinogradova & Plyusnina 1967). Babingtonite from the same sample as the ilvaite in Table 1 has lower $Fe^{2+}/(Fe^{2+} + Mg)$ and $Fe^{2+}/(Fe^{2+} + Mn)$ ratios (0.86 and 0.84, respectively) than the ilvaite (0.95 and 0.93), suggesting that both Mg and Mn substitute preferentially in babingtonite relative to ilvaite. The ilvaite and babingtonite are not in textural equilibrium, so that partition coefficients for this pair may not reflect chemical equilibrium conditions. Cell refinement based on X-ray powder patterns of the babingtonite give the following data: a 7.49(1), b 11.83(1), c 6.72(1) Å, α 95.3(1)°, β 92.3(1)° and γ 103.1(1)°. Optical data are n_α = 1.716(2), n_β = 1.731(2), n_γ = 1.750(2), $Z\Lambda c$ = 43(3)° and $2V_\alpha$ = 69(3)°.

Actinolite (Table 1, No. 6) is the most magnesian of the minerals analyzed, and stilpnomelane (Table 1, No. 7) is the only mineral containing K_2O in other than trace amounts. The composition of epidote in the skarns has been determined by X-ray diffraction (Hörmann & Raith 1971). Epidotes from eight samples of epidote skarn show a progressive decrease in Fe_2O_3 (and hence an increase in Al_2O_3) from 19.3 wt. % within the Ca–Fe–Si skarn to 11.7 wt. % at the metaclastic rock contact. Similar relationships have been described from skarns in Japan by Ito (1962) and Shimazaki (1969).

In the Ca–Fe–Si skarns, the minerals analyzed, with the exception of the minor phases actinolite, stilpnomelane and epidote, approach Ca–Fe end-members; the additional components, namely, Al_2O_3, MgO and MnO, generally amount to less than 5% of the totals. Minerals with such nearly end-member compositions as those at Black Perry Mountain are relatively uncommon in skarns. Many Fe-rich skarns contain appreciable Al_2O_3 and MgO, so that pyroxenes are salites or ferrosalites, and grossular-rich garnet tends to be the dominant garnet species. Also, other minerals such as idocrase and epidote may be present in considerable amounts (*e.g.*, Brock 1972, Morgan 1975, Kwak 1978). That babingtonite is not more common in Fe-rich skarns is probably due, in large measure, to the presence of components other than Ca, Fe, Mn, Si, O and H (Burt 1971a). Skarns with a mineralogy similar to that of the Black Perry Mountain skarns, although not always containing babingtonite,

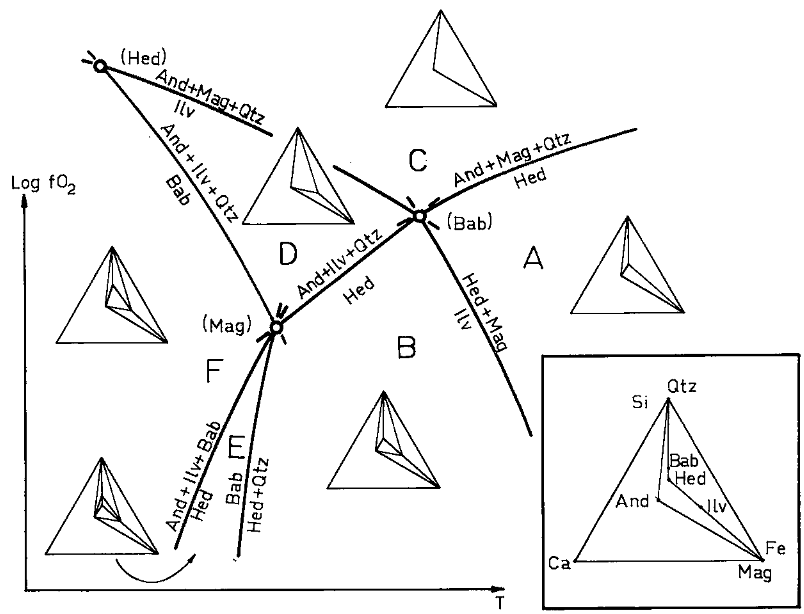

FIG. 3. Schematic, isobaric $f(O_2)$–T diagram involving Hed–And–Ilv–Bab–Mag–Qtz modified from Burt (1971a). Abbreviations as in Table 2. The invariant points are named by the absent phase. Letters represent stability fields of the equilibrium mineral-assemblages in Table 3.

TABLE 2. MINERAL FORMULAE AND ABBREVIATIONS

Ferro-actinolite	Act	$Ca_2Fe_5^{2+}Si_8O_{23}(OH)_2$
Andradite	And	$Ca_3Fe_2{}^{3+}Si_3O_{12}$
Babingtonite	Bab	$Ca_2Fe^{2+}Fe^{3+}Si_5O_{14}(OH)$
Calcite	Cal	$CaCO_3$
Hedenbergite	Hed	$CaFe^{2+}Si_2O_6$
Ilvaite	Ilv	$CaFe_2{}^{2+}Fe^{3+}Si_2O_8(OH)$
Magnetite	Mag	Fe_3O_4
Quartz	Qtz	SiO_2
Wollastonite	Woll	$CaSiO_3$

have been described by Schmitt (1939), Ito (1962), Bartholomé & Dimanche (1967), Shimazaki (1969) and Burt (1971b), among others.

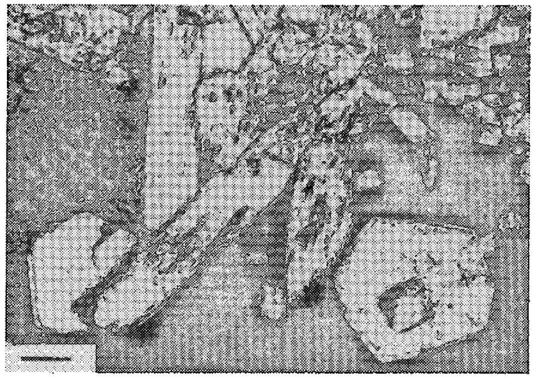

FIG. 4. An intergrowth of andradite, hedenbergite and babingtonite (dark grey and black) showing sharp grain boundaries between phases. The clear patch is a hole. The texture is interpreted as indicating that andradite, hedenbergite and babingtonite are in mutual chemical equilibrium. Hedenbergite shows partial replacement by actinolite. Plane-polarized light. Scale bar: 0.1 mm.

PHASE DIAGRAMS

Phase diagrams for part of the system Ca–Fe–Si–C–O–H relevant to Black Perry rocks have been constructed by Burt (1971a, b, c), Gustafson (1974), Liou (1974) and Taylor & Liou (1978). Figure 3 is a schematic, isobaric $f(O_2)$–T diagram involving the minerals hedenbergite, andradite, ilvaite, babingtonite, magnetite and quartz. Mineral formulae and abbreviations are listed in Table 2. Reactions involving CO_2 are not represented in Figure 3, although calcite can be regarded as stable within the conditions represented by the diagram (Burt 1971a).

TEXTURES AND ASSEMBLAGES

At Black Perry Mountain the main minerals within the assemblage And–Hed–Bab have sharp grain boundaries with each other (Fig. 4). The occurrence of andradite grains showing well-formed crystal faces and of hedenbergite grains showing elongate prism faces as inclusions in babingtonite is interpreted as indicating that these minerals grew simultaneously; therefore, they are assumed to have approached mutual chemical equilibrium. This interpretation is complicated by the compositional zoning in the garnets, although this is unlikely to affect greatly the discussion and conclusions below.

Based on textural observations similar to those above (*i.e.*, sharp, "clean" grain boundaries, well-formed crystal faces, minerals in contact with all others in the assemblage), assemblages listed in Table 3 are interpreted as being in equilibrium. Only the lowest-variance assemblages are cited. With the exception of And–Mag–Qtz (observed only in boulders) and babingtonite-bearing assemblages, the assemblages cited in Table 3 occur in all Ca–Fe–Si skarn outcrops. And–Hed–Qtz±Cal, which is by far the most common low-variance assemblage, is stable in fields A and B in Figure 3, And–Mag–Qtz is stable in field C, And–Ilv–Qtz–Cal in field D, Bab–And–Hed in field E and Bab–Qtz–Cal in fields E and F. The assemblages Act–And, Act–Ilv and Act–Mag are probably also equilibrium assemblages. Although the grain boundaries in these assemblages are ragged, the minerals occur in well-defined veinlets and probably approach mutual chemical equilibrium.

Textures that indicate the breakdown of hedenbergite to andradite, such as ragged hedenbergite inclusions in andradite (Fig. 5), are ubiquitous. Evidence for the breakdown of Hed ± Qtz to ilvaite, magnetite (Fig. 6) or actinolite is also widespread, whereas textures with Hed + Mag and And + Qtz overprinted by ilvaite occur only at a few localities. Only rarely is calcite seen transgressing or being transgressed by other minerals. Commonly, where calcite does occur in such reaction textures, hedenbergite is also involved and is seen to be breaking down, *e.g.*, Hed → Cal + Mag, Hed +

TABLE 3. ASSEMBLAGES INTERPRETED ON TEXTURAL GROUNDS TO APPROACH CHEMICAL EQUILIBRIUM

And-Hed-Qtz-Cal, And-Ilv-Qtz-Cal, And-Mag-Qtz, Bab-And-Hed, Bab-Otz-Cal.

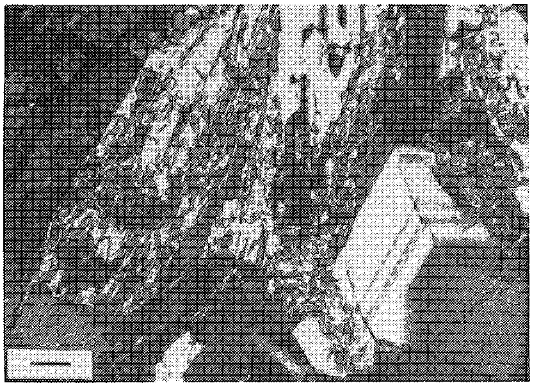

FIG. 5. Hedenbergite–andradite intergrowth in which andradite embays and transgresses otherwise tabular hedenbergite grains. Hedenbergite–andradite grain boundaries are generally ragged. Crossed nicols. Scale bar: 0.1 mm.

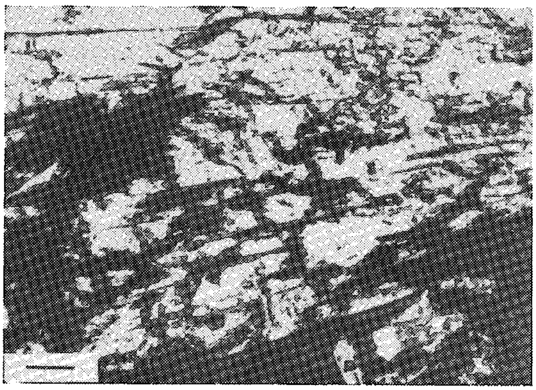

FIG. 6. Magnetite (black) along the cleavage of hedenbergite embaying and transgressing otherwise tabular grains. Most magnetite in the Ca–Fe–Si rocks occurs in intergrowths similar to that shown in this microphotomicrograph. Plane-polarized light. Scale bar: 0.2 mm.

Qtz → And + Cal, Hed + Cal → Ilv, Hed → Cal + Qtz + Bab. Other textures involving calcite are Ilv + epidote → Bab + Cal, And → Qtz + Cal and Cal → stilpnomelane.

Important relationships shown by the above textures are: (1) magnetite, ilvaite, babingtonite and actinolite always appear to be later than hedenbergite; (2) ilvaite is later than magnetite, and (3) babingtonite is later than ilvaite.

Most of the reaction textures, which occur on a thin-section scale, cannot be represented by balanced reactions involving the minerals present in the textures, O_2, H_2O and CO_2. Components such as Ca, Fe and Si also are involved. These reactions thus appear to be open on a scale at least larger than that of a thin section. The very large number of possible reactions involving the minerals at Black Perry Mountain and components of a C–O–H fluid makes it difficult to assign a particular partial-reaction texture to reactions such as those in Figure 3 or in the μ–μ diagrams constructed by Burt (1971a, b, c). Based on the textural and assemblage data, Figure 3 can, therefore, be used only in a general way to depict the changes in metamorphic conditions that occurred as the skarns cooled after their formation.

METAMORPHIC CONDITIONS

Although direct evidence of metamorphic pressure was not obtained in this study, the geological setting (Adamson 1955, Ashley *et al.* 1971) suggests that the granite may be a high-level intrusion; a pressure of 1.5 ± 1 kbar is probable. With the uncertainty of the pressure estimate and unknown fluid composition, the presence of wollastonite northwest of Black Perry Mountain indicates a temperature of perhaps 500 to 650°C (Greenwood 1967) for this locality. Although this temperature estimate is poorly constrained, it does indicate that moderately high temperatures were reached near the centre of the metasedimentary embayment during contact metamorphism.

Hed–And–Qtz–Cal is stable within a narrow $f(O_2)$–T field lying above the upper $f(O_2)$ stability of graphite (Burt 1971c). Both the high- and low-temperature boundaries of this stability field are defined by reactions involving CO_2 (Burt 1971c). The high-temperature boundary-reaction is Qtz + Cal = Woll, and the low-temperature boundary-reaction is And = Hed + Cal + Mag. The position of the stability field will thus depend on the $X(CO_2)$ of the metamorphic fluid. The relative T–$X(CO_2)$ stabilities of hedenbergite, andradite, quartz, calcite and wollastonite within the pure Ca–Fe–Si system at 2 kbar and log $f(O_2) = -18.5$ (Fig. 7) indicate that Hed–And–Qtz–Cal is stable at $X(CO_2)$ values between about 0.1 and 0.3 and at temperatures between approximately 580 and 640°C. Assuming $X(CO_2) = 0.25$, the T–$f(O_2)$ location of the stability field lies between log $f(O_2)$ values of 10^{-16} and $10^{-18.5}$ and about 550 to 610°C (Fig. 8).

The patchy distribution of reaction products indicates that reactions within local mineral-assemblages have been the dominant factor in controlling the chemical potentials of fluid com-

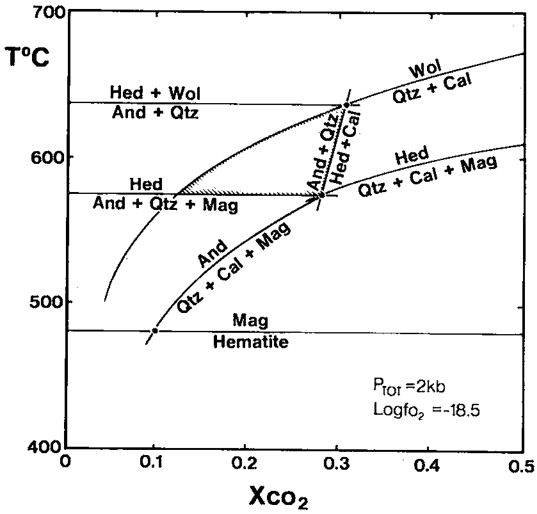

FIG. 7. T–$X(CO_2)$ diagram at P_{fluid} = 2 kbar and log $f(O_2)$ = −18.5 (modified from Taylor & Liou 1978). The hatched area represents the stability field of Hed–And–Qtz–Cal. The reaction Qtz + Cal = Woll is from Greenwood (1967), Hed = And + Qtz + Mag from Gustafson (1974), And + Qtz = Hed + Woll and Hed + Cal = And + Qtz from Liou (1974), And = Qtz + Cal + Mag and Hed = Qtz + Cal + Mag from Taylor & Liou (1978).

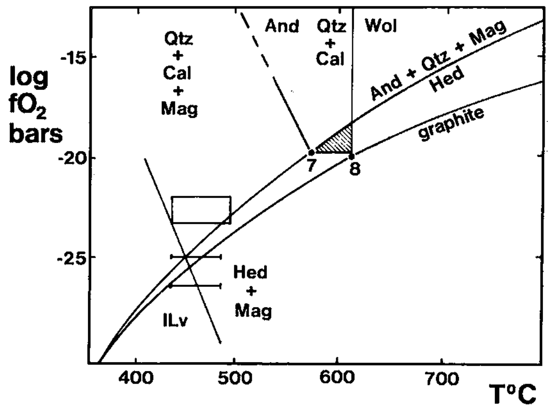

FIG. 8. $f(O_2)$–T diagram showing experimentally determined reactions at 2 kbar applicable to Black Perry rocks. Hed = And + Mag + Qtz and Hed + Mag = Ilv reactions from Gustafson (1974). Bars represent experimental error of the Hed + Mag = Ilv reaction, and the rectangle represents experimental uncertainty for the (Bab) invariant point in Figure 3. Qtz + Cal = Woll reaction, assuming $X(CO_2)$ = 0.25, from Greenwood (1967). The curve for graphite is from Huebner (1971). The invariant points 7 and 8 are identical to those in Figure 39 of Burt (1971c) and Figure 7 of Liou (1974). The hatched area represents conditions in which the assemblage Hed–And–Qtz–Cal is stable. At lower $f(O_2)$ values, calcite and andradite are not compatible (Burt 1971b, Liou 1974, Taylor & Liou 1978). Below about 500°C, the relative positions of the curves for the Hed = And + Mag + Qtz reaction and graphite are uncertain (Gustafson 1974).

ponents rather than these being determined externally (Kerrick 1974, Kerrick *et al.* 1973). The ubiquitous reaction-textures involving hedenbergite suggest that in most Ca–Fe–Si rocks, the volume of hedenbergite relative to the volume of fluids migrating through the rocks was such that the buffering capacity of the hedenbergite-breakdown reactions was not exceeded. However, the occurrence of assemblages that are stable outside fields A and B in Figure 3 (see Table 3) suggests that the hedenbergite-breakdown reactions were exhausted locally owing to the complete consumption of hedenbergite.

The restricted occurrence of babingtonite in the field indicates that conditions not experienced elsewhere in the rocks existed at these localities. Relationships in chemical potential diagrams suggest that babingtonite, relative to ilvaite, requires hydrous conditions and, in systems where CO_2 is a mobile component, also requires relatively low $X(CO_2)$ in the fluid phase (Burt 1971a). The temperature at which babingtonite first forms is somewhat below that at which ilvaite can form (Fig. 3).

Burt (1971a) suggested that end-member ferroactinolite forms at $f(O_2)$ values below the (Mag) and (Bab) invariant points in Figure 3. The magnesian composition of the actinolite at Black Perry Mountain, together with the Fe^{2+}- and Fe^{3+}-rich composition of coexisting minerals, suggest that the actinolite formed under relatively oxidizing conditions. Its stability field within Figure 3 is uncertain, although it would cover a wide field in this diagram.

The interpreted paragenetic sequence, together with the stability fields defined by the equilibrium assemblages (Table 3), suggest that at least in some parts of the Ca–Fe–Si skarn, T–$f(O_2)$ conditions moved from field A in Figure 3 to fields E and F as the rocks cooled from the peak metamorphic conditions.

In the epidote skarns, the systematic variation in epidote compositions from the Ca–Fe–Si skarns to the metasediment suggests that there has been diffusion across the contact between these contrasting rock-types, as has been proposed for other epidote skarns with similar characteristics (Ito 1962).

SUMMARY

(1) In an embayment into an intrusive granite, extensive outcrops of Ca–Fe–Si skarn contain similar assemblages of minerals in which the main minerals have nearly end-member compositions. Babingtonite is the only mineral restricted in its occurrence.

(2) During emplacement of the granite, interaction between marble and metasomatic fluids formed Ca–Fe–Si skarns in which Hed–And–Qtz–Cal is the stable assemblage. All presently exposed skarns experienced generally similar peak contact-metamorphic conditions of 580 to 640°C, $X(CO_2)$ of 0.1 to 0.3 and with $f(O_2)$ just above the upper $f(O_2)$ stability of graphite. The granite is thus probably buried not too deeply below the embayment.

(3) During subsequent cooling of the Ca–Fe–Si skarn, an O–H fluid was buffered by hedenbergite-breakdown reactions within local mineral-assemblages, although in places these buffer reactions were exhausted. At a very few localities, reactions involved a C–O–H fluid.

(4) At only a very few localities was the fluid buffered to compositions that would allow babingtonite to form.

ACKNOWLEDGEMENTS

Drs. R.H. Flood, T.H. Green and R.H. Vernon are thanked for suggesting the study of the Black Perry Mountain rocks and for their assistance during the project. Dr. R.A. Binns read an early draft. Constructive reviews by Drs. L.J. Cabri, E.C. Appleyard and two anonymous reviewers are acknowledged.

REFERENCES

ADAMSON, C.L. (1955): Reconnaissance geology of the Snowy Mountains area. Progress report II: Yarrangobilly. *Tech Rep. Dep. Mines New South Wales* **3**, 34-42.

ASHLEY, P.M., CHENHALL, B.E., CREMER, P.L. & IRVING, A.J. (1971): The geology of the Coolac serpentinite and adjacent rocks east of Tumut, New South Wales. *J. Proc. Roy. Soc. New South Wales* **104**, 11-28.

BARTHOLOMÉ, P. & DIMANCHE, F. (1967): On the paragenesis of ilvaite in Italian skarns. *Ann. Soc. Géol. Belg.* **90**, 533-563.

BENCE, A.E. & ALBEE, A.L. (1968): Empirical correction factors for the electron microanalysis of silicates and oxides. *J. Geol.* **76**, 382-403.

BROCK, K.J. (1972): Genesis of Garnet Hill skarn, Calaveras County, California. *Geol. Soc. Amer. Bull.* **83**, 3391-3404.

BURT, D.M. (1971a): On the paragenesis of babingtonite. *Soc. Mining Geol. Japan. Spec. Issue* **3**, 375-380.

——— (1971b): The facies of some Ca–Fe–Si skarns in Japan. *Carnegie Inst. Wash. Year Book* **70**, 185-188.

——— (1971c): Some phase equilibria in the system Ca–Fe–Si–C–O. *Carnegie Inst. Wash. Year Book* **70**, 178-184.

——— (1974): Metasomatic zoning in Ca–Fe–Si exoskarns. *In* Geochemical Transport and Kinetics (A.W. Hofmann, B.J. Giletti, H.S. Yoder, Jr. & R.A. Yund, eds.). *Carnegie Inst. Wash. Publ.* **634**, 289-293.

GREENWOOD, H.J. (1967): Wollastonite: stability in H_2O–CO_2 mixtures and occurrence in a contact-metamorphic aureole near Salmo, British Columbia, Canada. *Amer. Mineral.* **52**, 1669-1680.

GUSTAFSON, W.I. (1974): The stability of andradite, hedenbergite and related minerals in the system Ca–Fe–Si–O–H. *J. Petrology* **15**, 455-496.

HÖRMANN, P.-K. & RAITH, M. (1971): Optische Daten, Gitterkonstanten, Dichte und magnetische Suszeptibilität von Al-Fe (III)-Epidoten. *Neues Jahrb. Mineral. Abh.* **116**, 41-60.

HUEBNER, J.S. (1971): Buffering techniques for hydrostatic systems at elevated pressures. *In* Research Techniques for High Pressure and High Temperature (G.C. Ulmer, ed.). Springer-Verlag, Heidelberg.

ITO, K. (1962): Zoned skarn of the Fujigaturi mine, Yamaguchi Prefecture. *Jap. J. Geol. Geog.* **33**, 169-190.

KERRICK, D.M. (1974): Review of metamorphic mixed volatile (H_2O–CO_2) equilibria. *Amer. Mineral.* **59**, 729-762.

———, CRAWFORD, K.E. & RANDAZZO, A.F. (1973): Metamorphism of calcareous rocks in three roof pendants in the Sierra Nevada, California. *J. Petrology* **14**, 303-325.

KWAK, T.A.P. (1978): Mass balance relationships and skarn-forming processes at the King Island scheelite deposit, King Island, Tasmania, Australia. *Amer. J. Sci.* **278**, 943-968.

LEONARD, B.F., HILDERBRAND, F.A. & VLISIDES, A.C. (1962): Members of the ludvigite – vonsenite series and their distinction from ilvaite. *In* Petrologic Studies: A Volume to Honor A.F. Buddington (A.E.J. Engel, H.L. James & B.F. Leonard, eds.). Geol. Soc. Amer., 523-568.

LIOU, J.G. (1974): Stability relations of andradite–quartz in the system Ca–Fe–Si–O–H. *Amer. Mineral.* **59**, 1016-1025.

MORGAN, B.A. (1975): Mineralogy and origin of skarns in the Mount Morrison pendant, Sierra Nevada, California. *Amer. J. Sci.* **275**, 119-142.

PAPIKE, J.J., CAMERON, K.L. & BALDWIN, K. (1974): Amphiboles and pyroxenes: characterization of *other* than quadrilateral components and estimates of ferric iron from microprobe data. *Geol. Soc. Amer. Abstr. Programs* **6**, 1053-1054.

SCHMITT, H. (1939): The Pewabic mine. *Geol. Soc. Amer. Bull.* **50**, 777-818.

SHIMAZAKI, H. (1969): Pyrometasomatic copper and iron ore deposits of the Yaguki mine, Fukushima Prefecture, Japan. *J. Fac. Sci., Univ. Tokyo (Sect. 2)* **17**, 317-350.

TAYLOR, B.E. & LIOU, J.G. (1978): The low-temperature stability of andradite in C–O–H fluids. *Amer. Mineral* **63**, 378-393.

VINOGRADOVA, R.A. & PLYUSNINA, I.I. (1967): Composition, properties and crystallochemical features of minerals in the isomorphic ferrobabingtonite–manganbabingtonite series. *Vestn. Mosk. Univ. (Ser. 4)* **22**(4), 56-67 (in Russ.).

Received November 1980, revised manuscript accepted February 1981.